American Journal of Engineering Research (AJER)
e-ISSN: 2320-0847 p-ISSN : 2320-0936
Volume-13, Issue-3, pp-20-29
www.ajer.org
Research Paper Open Access

Particle Swarm Optimization Based Unified Power Flow Controller Placement For Power System Loss Minimization

[1*]Ogunbowale, P. E., [2]Adejumobi, I. A., [3]Adebisi, O. I. and [4]Osinuga, I. A.
[1,2,3] *Department of Electrical and Electronics Engineering, Federal University of Agriculture, Abeokuta, Ogun State, Nigeria*
[4] *Department of Mathematics, Federal University of Agriculture, Abeokuta, Ogun State, Nigeria*
**Corresponding Author E-mail: ogunbowalepeter@gmail.com*

ABSTRACT: *Over the last two decades, the size and complexity of electric power system has increased due to large demand for electricity, which causes the power systems to operate close to their thermal and stability limits and the consequences of which are power outages, high line losses, poor bus voltages, total blackouts among others. This work employed particle swarm optimization (PSO) based unified power flow controller (UPFC) placement for power system loss minimization using the IEEE 30-bus system as a test network. The load flow equations were formulated modeling the steady state performance of the power system using Gauss-Seidel iterative method, modified through inclusion of unified power flow controller, and simulated using particle swarm optimization algorithm without and with compensation in Python environment (version 3.7). The line with the least active power loss was used to determine the optimum point for unified power flow controller location, and* $0.95 \leq V \leq 1.10$ *p.u defined as the voltage statutory limit. The obtained results showed that line 12-13 was the optimal point, and all the voltage profile were within the statutory limit without and with unified power flow controller placed at the optimal point, the total active power loss in the system reduced from 499.1 to 206.4 MW, given reduction of 58.65 %, while the total reactive power loss reduced from 2488.7 to 2067.2 MVAr with reduction of 16.94 %. These results showed that PSO based UPFC placement is suitable and appropriate for both voltage stability enhancement and power loss minimization.*
KEYWORDS: *FACTS, Gauss-Seidel method, power loss, PSO algorithm, UPFC, voltage profile*

Date of Submission: 01-03-2024 Date of acceptance: 09-03-2024

I. INTRODUCTION

The electricity grid is a complex network consisting of transmission lines, generators, transformers, circuit breakers, bus bars, isolators, loads among others. Nowadays, the demand for power supply has drastically increased due to increase in population and technological development, creating a demand-supply electricity gap resulting in system instability, high transmission losses, poor power quality, persistent system collapse among others. This demand-supply shortfall has put power system engineers on their toes to find a permanent solution to various issues surrounding the unavailability of power supply [1].

One way of ensuring there is proper balance between power generated and load is by establishing more generating plants, constructing alternative or new transmission lines among others, which will provide stable, secure and improvement in electricity supply. But cost limitations, environmental restrictions, land acquisition challenge, among others have made power supply providers to seek an alternative solution to shortage of electricity. Another approach of closing the demand-supply electricity gap is by using reactors to stabilize the power system when it is lightly loaded, and capacitor banks during system overloading to compensate for shortage of reactive power, and in some cases resort to load shedding. But this method of power compensation and control suffers wear and tear due to its moving parts [1], [2], [3], [4].

Recent development has been tilted towards the use of Flexible Alternating Current Transmission System (FACTS) devices to optimize the available capacity, as previous methods proved ineffective. Hence, there is need for extensive research on its use and should be given the needed priority.

FACTS devices help to reduce power flow congestion in an overloaded line, minimize power losses, boost voltage profile, ensure security of supply, efficient use of the existing transmission network, and ensure that the power system control parameters fall within the constraints limits [5]. Therefore, this study employed PSO based UPFC placement for power system loss minimization. UPFC is a costly device, and it is important that it is optimally located on the power system network to maximize its capacity.

II. MATERIALS AND METHODS

3.1 Formulation of Load Flow Equations

A power system network consists of a generator, load and transmission lines interconnected together, and a typical representation is shown in Figure 1.

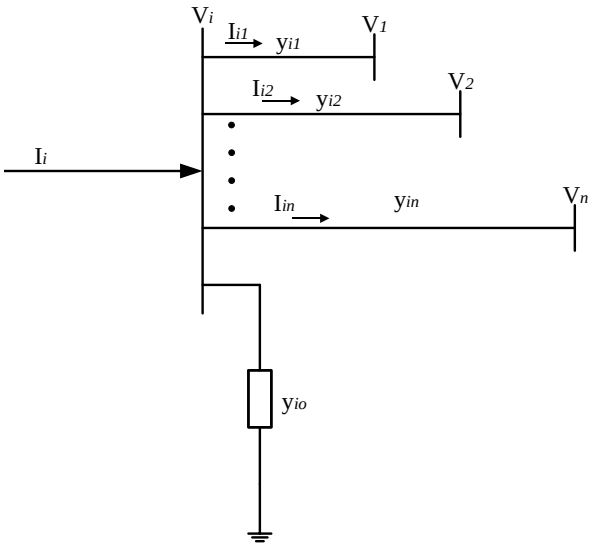

Figure 1: A transmission line model

Applying Kirchhoff's current law to bus i in Figure 1 gives equation (1):

$$I_i = I_{i0} + I_{i1} + I_{i2} + \cdots + I_{iN} \tag{1}$$

The sum-total nodal current (I_i) of bus i in Figure 1 can be written as equation (2) with the use of Ohm's law, and rearranging equation (2) gives equation (3):

$$I_i = y_{i0}V_i + y_{i1}(V_i - V_1) + y_{i2}(V_i - V_2) + \cdots + y_{iN}(V_1 - V_N) \tag{2}$$

$$I_i = (y_{i0} + y_{i1} + y_{i2} + \cdots + y_{iN})V_i - y_{i1}V_1 - y_{i2}V_2 - \cdots - y_{iN}V_N \tag{3}$$

The self-admittance (Y_{ii}) and mutual admittance (Y_{ik}) between bus i and k, is defined by equation (4):

$$\left.\begin{aligned} Y_{ii} &= y_{i0} + y_{i1} + y_{i2} + \cdots + y_{iN} \\ Y_{i1} &= -y_{i1} \\ Y_{i2} &= -y_{i2} \\ &\vdots \quad \vdots \quad \vdots \\ Y_{iN} &= -y_{iN} \end{aligned}\right\} \tag{4}$$

By substituting equation (4) into equation (3) gives equation (6):

$$I_i = Y_{ii}V_i + Y_{i1}V_1 + Y_{i2}V_2 + \cdots + Y_{iN}V_N \tag{5}$$

$$I_i = Y_{ii}V_i + \sum_{\substack{k=1 \\ k \neq i}} Y_{ik}V_k \tag{6}$$

The injected complex power at bus i is expressed as equation (7) [6]:

$$S_i = P_i + jQ_i = V_i I_i^* \tag{7}$$

Taking the complex conjugate of equation (7) gives equation (8), and substituting equation (6) into equation (8) gives equation (10):

$$S_i^* = P_i - jQ_i = V_i^* I_i \tag{8}$$

$$\frac{P_i - jQ_i}{V_i^*} = I_i \tag{9}$$

$$\frac{P_i - jQ_i}{V_i^*} = Y_{ii}V_i + \sum_{\substack{k=1 \\ k \neq i}}^{N} Y_{ik}V_k \tag{10}$$

Making V_i the subject of the formula in equation (10) gives equation (11), which is the Gauss-Seidel load flow equation, and the iteration for Gauss-Seidel method is given by equation (12):

$$V_i = \frac{1}{Y_{ii}}\left[\frac{P_i - jQ_i}{V_i^*} - \sum_{\substack{k=1 \\ k \neq i}}^{N} Y_{ik}V_k\right]; \quad i = 2, 3, ..., N \tag{11}$$

$$V_i^{r+1} = \frac{1}{Y_{ii}}\left[\frac{P_i - jQ_i}{\left(V_i^r\right)^*} - \sum_{\substack{k=1 \\ k \neq i}}^{N} Y_{ik}V_k^r\right]; \quad i = 2, 3, ..., N \tag{12}$$

By separating equation (11) into real and imaginary parts produced the quadratic equations (13) and (14) respectively:

$$P_i = |V_i|^2 G_{ii} + \sum_{\substack{k=1 \\ k \neq i}}^{N} |Y_{ik}V_iV_k| cos\left(\theta_{ik} + \delta_k - \delta_i\right) \tag{13}$$

$$Q_i = |V_i|^2 B_{ii} + \sum_{\substack{k=1 \\ k \neq i}}^{N} |Y_{ik}V_iV_k| sin\left(\theta_{ik} + \delta_k - \delta_i\right) \tag{14}$$

where P_i and Q_i are real and reactive power, I_i^* and V_i^* are complex conjugate of bus i current and voltage, i is the number of buses, r is the number of iterations, G_{ii} is self-conductance, B_{ii} is self-susceptance, δ_i is phase angle, and θ_{ik} is phase difference between admittance of bus i and admittance of bus j.

The net value of active and reactive power at bus i are calculated using equation (15), and the voltage-drop on the line between bus i and k can be calculated using equation (16):

$$\left.\begin{aligned} P_i &= P_{G,i} - P_{D,i} \\ Q_i &= Q_{G,i} - Q_{D,i} \end{aligned}\right\} \tag{15}$$

$$\Delta V_{ik} = |V_i - V_K| \tag{16}$$

where P_i and Q_i are net value of active and reactive power, $P_{G,i}$ and $Q_{G,i}$ are power generated, $P_{D,i}$ and $Q_{D,i}$ are power demand, and ΔV_{ik} is voltage drop between bus i and k

The mathematical manipulation of equations (7) and (16) give equations (17) and (18) respectively, which is the real and reactive line losses between bus i and k:

$$P_{Lik} = G_{ik}\left(V_i^2 + V_k^2 - 2V_iV_k\cos\theta_m\right) \tag{17}$$

$$Q_{Lik} = -V_i^2 B_{ik} - V_k^2 B_{ik} - 2B_{ik}V_iV_k\cos\theta_m \tag{18}$$

3.2 Modelling of UPFC into the Load Flow Equations

Figure 2 shows the UPFC model equivalent circuit, and is expressed by equations (19) to (28) [7]:

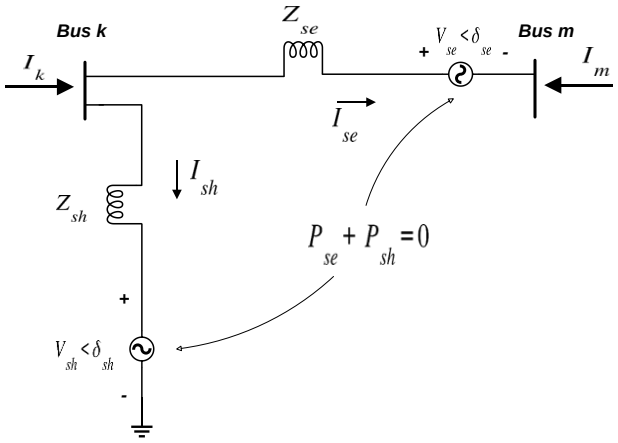

Figure 2: UPFC model

From Figure 2, subscript se and sh representing series and shunt respectively. The shunt (E_{sh}) and series (E_{se}) voltage sources are given by equations (19) and (20) respectively:

$$E_{sh} = V_{sh}\left(\cos\delta_{sh} + j\sin\delta_{sh}\right) \quad (19)$$

$$E_{se} = V_{se}\left(\cos\delta_{se} + j\sin\delta_{se}\right) \quad (20)$$

where V_{sh} , V_{se} is controllable voltage magnitude, and δ_{sh}, δ_{se} is controllable phase angle with constraint of $\left(V_{min} \le V \le V_{max}\right)$ and $\left(0 \le \delta \le 2\pi\right)$ respectively.

The real and reactive power equations at bus k are given by equations (21) and (22), and at bus m, are given by equations (23) and (24) respectively:

$$P_k = V_k^2 G_{kk} + V_k V_m\left[G_{km}\cos\left(\theta_k - \theta_m\right) + B_{km}\sin\left(\theta_k - \theta_m\right)\right] + V_k V_{se}\left[G_{km}\cos\left(\theta_k - \delta_{se}\right) + B_{km}\sin\left(\theta_k - \delta_{se}\right)\right] + V_k V_{sh}\left[G_{sh}\cos\left(\theta_k - \delta_{sh}\right) + B_{sh}\sin\left(\theta_k - \delta_{sh}\right)\right] \quad (21)$$

$$Q_k = -V_k^2 B_{kk} + V_k V_m\left[G_{km}\sin\left(\theta_k - \theta_m\right) - B_{km}\cos\left(\theta_k - \theta_m\right)\right] + V_k V_{se}\left[G_{km}\sin\left(\theta_k - \delta_{se}\right) - B_{km}\cos\left(\theta_k - \delta_{se}\right)\right] + V_k V_{sh}\left[G_{sh}\sin\left(\theta_k - \delta_{sh}\right) - B_{sh}\cos\left(\theta_k - \delta_{sh}\right)\right] \quad (22)$$

$$P_m = V_m^2 G_{mm} + V_m V_k\left[G_{mk}\cos\left(\theta_m - \theta_k\right) + B_{mk}\sin\left(\theta_m - \theta_k\right)\right] + V_m V_{se}\left[G_{mm}\cos\left(\theta_m - \delta_{se}\right) + B_{mm}\sin\left(\theta_m - \delta_{se}\right)\right] \quad (23)$$

$$Q_m = -V_m^2 B_{mm} + V_m V_k\left[G_{mk}\sin\left(\theta_m - \theta_k\right) - B_{mk}\cos\left(\theta_m - \theta_k\right)\right] + V_m V_{se}\left[G_{mm}\sin\left(\theta_m - \delta_{se}\right) + B_{mm}\cos\left(\theta_m - \delta_{se}\right)\right] \quad (24)$$

The active and reactive power equations for series converter are given by equations (25) and (26), and for shunt converter are given by equations (27) and (28) respectively:

$$P_{se} = V_{se}^2 G_{mm} + V_{se} V_k\left[G_{km}\cos\left(\delta_{se} - \theta_k\right) + B_{km}\sin\left(\delta_{se} - \theta_k\right)\right] + V_{se} V_m\left[G_{mm}\cos\left(\delta_{se} - \delta_m\right) + B_{mm}\sin\left(\delta_{se} - \theta_m\right)\right] \quad (25)$$

$$Q_{se} = -V_{se}^2 B_{mm} + V_{se} V_k\left[G_{km}\sin\left(\delta_{se} - \theta_k\right) - B_{km}\cos\left(\delta_{se} - \theta_k\right)\right] + V_{se} V_m\left[G_{mm}\sin\left(\delta_{se} - \theta_m\right) - B_{mm}\cos\left(\delta_{se} - \theta_m\right)\right] \quad (26)$$

$$P_{sh} = -V_{sh}^2 G_{sh} + V_{sh} V_k\left[G_{sh}\cos\left(\delta_{sh} - \theta_k\right) + B_{sh}\sin\left(\delta_{sh} - \theta_k\right)\right] \quad (27)$$

$$Q_{sh} = V_{sh}^2 B_{sh} + V_{sh} V_k\left[G_{sh}\sin\left(\delta_{sh} - \theta_k\right) - B_{sh}\cos\left(\delta_{sh} - \theta_k\right)\right] \quad (28)$$

3.3 Mathematical Model of PSO

PSO was modelled after the social behaviour of fish schooling [8]. This stochastic optimization technique uses a swarm of particles to find the optimal solution. Each particle is defined by a position and a velocity vector in a search space and communicate with each other to find solution to the problem. During the search process, each candidate keeps a record of its best location and tried to find a better position by updating its velocity [9]. The best location found by each candidate/particle is known as personal/particle best (P_{best}), while the best location found in the swarm among the particle is known as global best (G_{best}). It should be noted that there is always a G_{best} amongst the P_{best} and each particle converges towards the global best position (G_{best}). Since the search process is defined in the x-y plane, the candidate's position is in (x, y) direction and velocity vector (V_x, V_y).

The velocity and position vector of the ith particle in a search space is given by equation (29) and equation (30) respectively [10]:

$$F_i = \left(F_{i1}, F_{i2}, F_{i3} \ldots F_{id}\right)^T \quad (29)$$

$$X_i = \left(X_{i1}, X_{i2}, X_{i3} \ldots X_{id}\right)^T \quad (30)$$

The best position found by each particle is given by equation (31), and each particle moves in the direction towards the best location in the swarm known as global best position (G_{best}) given by equation (32):

$$P_{best\,i} = \left(P_{best\,i1}, P_{best\,i2}, P_{best\,i3} \ldots P_{best\,id}\right)^T \quad (31)$$

$$G_{best\,i} = \left(G_{best\,i1}, G_{best\,i2}, G_{best\,i3} \ldots G_{best\,id}\right)^T \quad (32)$$

Since velocity is the distance covered per unit time in a specified direction, each particle's new position is defined by a velocity which changes from time to time as particles move towards their personal best location (P_{best}) and global best position (G_{best}). The particle's velocity and position are updated based on the particle best and global best position found and are given by equation (33) and equation (34) respectively [11], [12]:

$$F_i^{k+1} = w \times F_i^k + c_1 \times r_1 \times \left(P_{best\,i} - x_i^k\right) + c_2 \times r_2 \times \left(G_{best\,i} - x_i^k\right) \quad (33)$$

$$x_i^{k+1} = x_i^k + LF_i^{k+1} \quad (34)$$

The maximum velocity (F_{max}) of the particles are restricted to prevent the particles from leaving the search space, while the minimum velocity ($-F_{max}$) are also restricted to prevent the particles from exploring below the local solution. The velocity of each particle falls between $-F_{max}$ to F_{max}.

The inertia weight is updated at each iteration and is given by equation (35) [13]:

$$w = w_{max} - \left(\left(w_{max} - w_{min}\right) \times k\right) / k_{max} \quad (35)$$

Where $x_i^{k+1}$and $F_i^{k+1}$are position and velocity of particle i at iteration k+1 (new value), x_i^k and F_i^k are position and velocity of particle i at iteration k (old value), $i = 1, 2, \ldots, N$ and $N$is swarm/population size, w is inertial weight of the particle, r_2 and r_1 are randomly generated numbers, c_2 and c_1 are acceleration constant, L is

constriction factor which ensure convergence, w_{min} and w_{max} are minimum and maximum inertia weight, k_{max} and k are maximum and current iteration.
A balance between the local and global exploration is provided by a good selection of inertia weight. Figure 3 show the particles behaviour in particle swarm optimization.

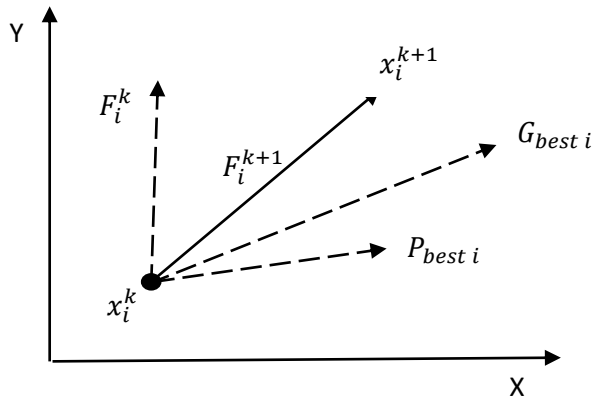

Figure 3: Particles' behaviour in particle swarm optimization

The location of UPFC depends on which transmission line with UPFC placement brings about the least active power loss among other lines in the power network. Therefore, the objective function is to find the optimum point for UPFC location which give the least active power loss, and is expressed as equation (36):

$$F_{obj} = min \sum_{i=1}^{NTL} P_{Loss} \quad (36)$$

Using equation (17) in equation (36) yields equation (37):

$$P_{Loss} = \sum_{i=1, j=1}^{NTL} G_{ij}\left(V_i^2 + V_j^2 - 2V_i V_j \cos(\theta_i - \theta_j)\right) \quad (37)$$

where P_{Loss} is active power loss, G_{ij} is conductance of line (i, j), $\theta_i - \theta_j$ is bus angle at bus i and j respectively, and NTL represents number of transmission lines. Subject to voltage constraints ($V_i^{min} \leq V_i \leq V_i^{max}$), branch current constraints ($I_{bij} \leq I_{bij}^{max}$), and power flow constraints.

From equation (33), make $G_{best\ i}$ the subject of the formula give equation (38):

$$G_{best\ i} = \frac{F_i^{k+1} - \left(w \times F_i^k + c_1 \times r_1 \times \left(P_{best\ i} - x_i^k\right)\right) + c_2 \times r_2 \times x_i^k}{c_2 \times r_2} \quad (38)$$

The global best (G_{best}) is directly proportional to objective function, and in this case, G_{best} is taken as the objective function value itself, and is expressed as equation (39):

$$G_{best} = min(P_{Loss}) \quad (39)$$

There is continuous iterative process in equations (33) and (34) until all the particles converge towards the G_{best}.

3.3.1 Optimal Placement of UPFC via PSO Algorithm

The solution procedures for particle swarm optimization are summarized as follows:

i. Input the bus data, generator data, line data and shunt data
ii. Size the UPFC device
iii. Read the bus data, generator data, line data and shunt data. Run the load flow analysis using Gauss-Seidel method and find the power losses and bus voltages
iv. Calculate the total line losses before the placement of UPFC device
v. Input the PSO parameter such as c_1 and c_2, r_1 and r_2, w among others. Maximum iteration is set as t = 100
vi. Generate randomly the initial search points (positions) and velocities of the particles with population size representing a solution to the objective function
vii. For each particle, evaluate their fitness function
viii. Find the optimal location for the UPFC device, where the least active power loss is recorded
ix. Each particle's position is assigned P_{best}. Find the G_{best} (i.e., where the least active power loss is observed)
x. Calculate the new-found position and velocity using equations (33), (34), and (35) respectively

xi. Continue to evaluate $Iteration = Iteration + 1$
xii. Check if $Iteration = Iteration_{max}$ (i.e., if the number of iterations reach the maximum limit) proceed to the next step, if not, go back to step xi
xiii. Set best of P_{best} as G_{best}
xiv. If G_{best} is the optimal solution proceed to step xv, otherwise, go back to step vi
xv. Calculate the total line losses and bus voltages after the placement of UPFC device
xvi. End

The implementation of all the derived load flow equations in this study is done through the application of PSO algorithm.

3.4 Choice of Simulation Software

In this work, the load flow code was developed in Python environment (version 3.7), and a jupyter notebook was used to run the Python code on windows 10 operating system. Jupyter notebook is an interactive way of running Python code, with high flexibility, rich formatting, and a great user interface. The notebooks are structured in cells where you write an entire program or lines of code and can be run one at a time or entirely. Python finds application in power networks, and it is easy to use, deploy with great library support.

3.5 Test Network

The test network used in this work was IEEE 30-bus system. The single line diagram of IEEE 30-Bus System is shown in Figure 4. It consists of thirty (30) buses and six (6) generation stations. The network and transmission line data were taken from [14], and the data is on 220kV and 100MVA base.

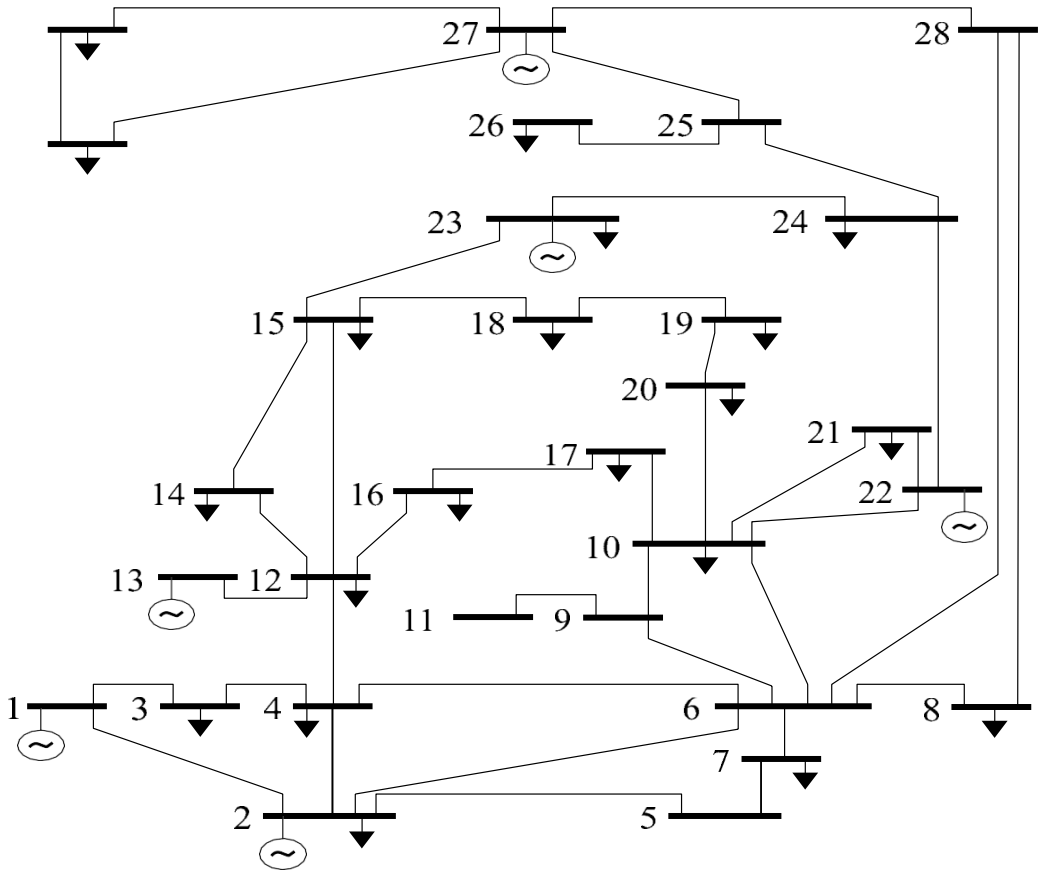

Figure 4: IEEE 30-bus power system [15]

III. RESULTS AND DISCUSSION

The load flow results without and with optimally placed UPFC device programmed in Python environment via the PSO algorithm, applied on the IEEE 30-bus power network are presented in this section. The parameters used for the PSO and UPFC sizing for the IEEE 30-bus power network is as attached in the appendix.

Active power loss is used as the selection criterion for optimal location of UPFC device on the power network. The PSO algorithm randomly select some of the lines with UPFC placement to show the effect of UPFC on different locations during the particle search. The particles converge at G_{best} location in which the effect of the compensation device (UPFC) would be maximally felt in terms of having the overall least real and reactive power losses and enhanced voltage profile on the considered network. The load flow results for IEEE 30-bus power network with UPFC placed on line 12-13 selected as the optimum point by the PSO algorithm are presented as follows:

Figure 5 shows UPFC placement at different locations on the IEEE 30-bus power network, while Figure 6 shows the comparison of the voltage profile without and with optimally placed UPFC device on line 12-13. Also, Figure 7 shows the comparison of the total active power loss without and with optimally placed UPFC, while Figure 8 shows the comparison of the total reactive power loss without and with optimally placed UPFC.

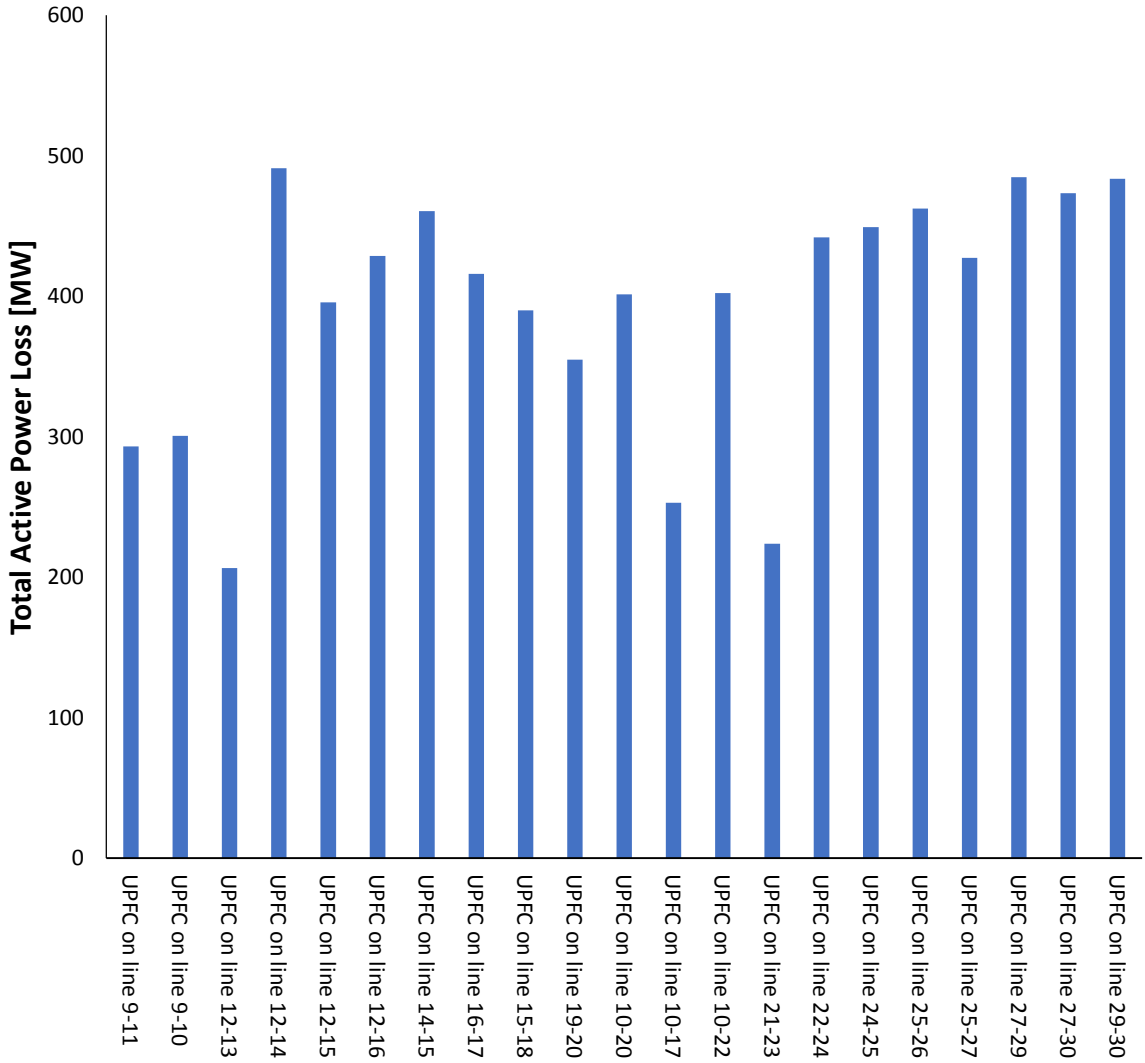

Figure 5: Total active power loss with UPFC placement at different locations on the IEEE 30-bus power system network

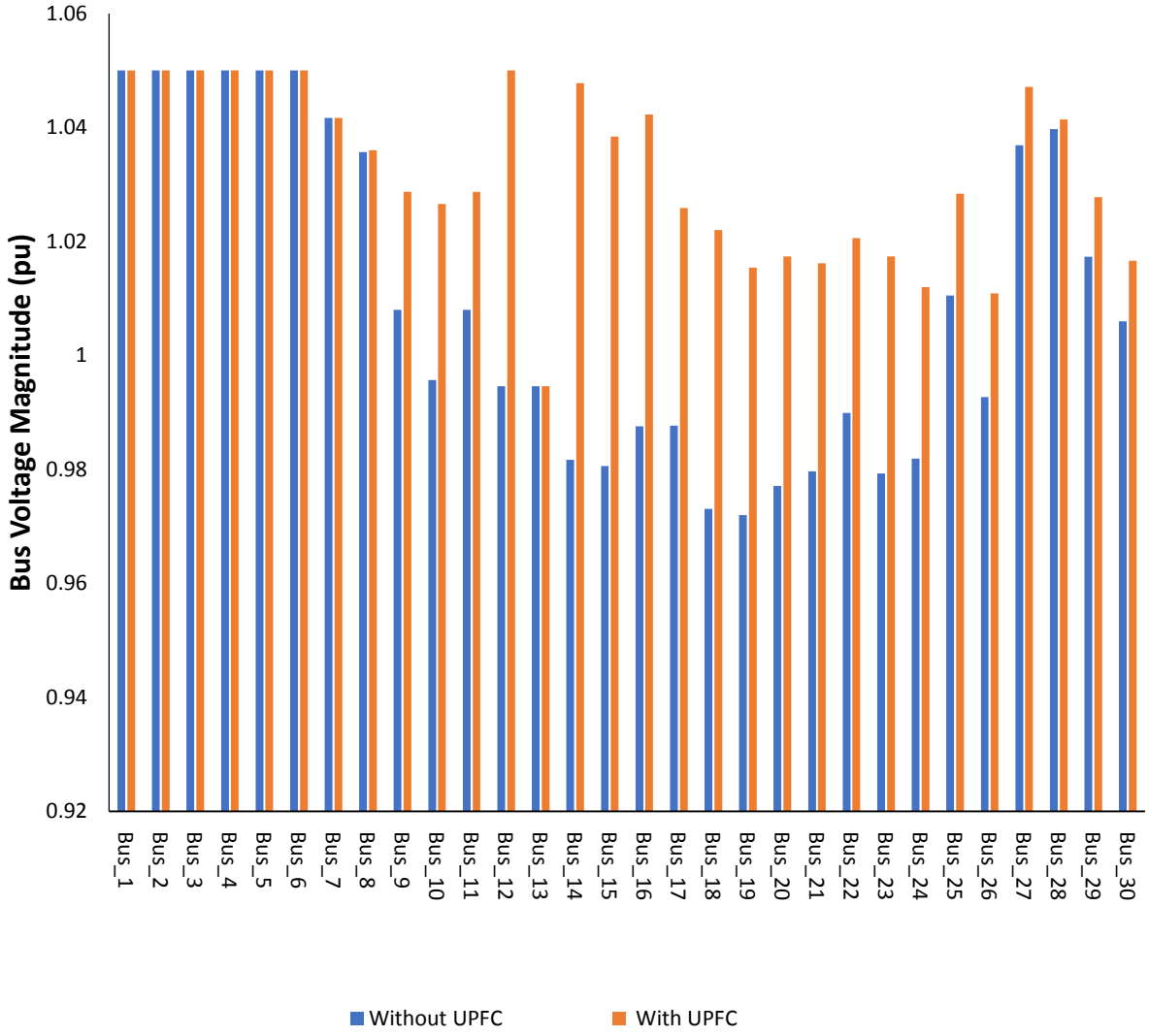

Figure 6: Comparison of bus voltage magnitudes without and with optimally placed UPFC device on the IEEE 30-bus power system network

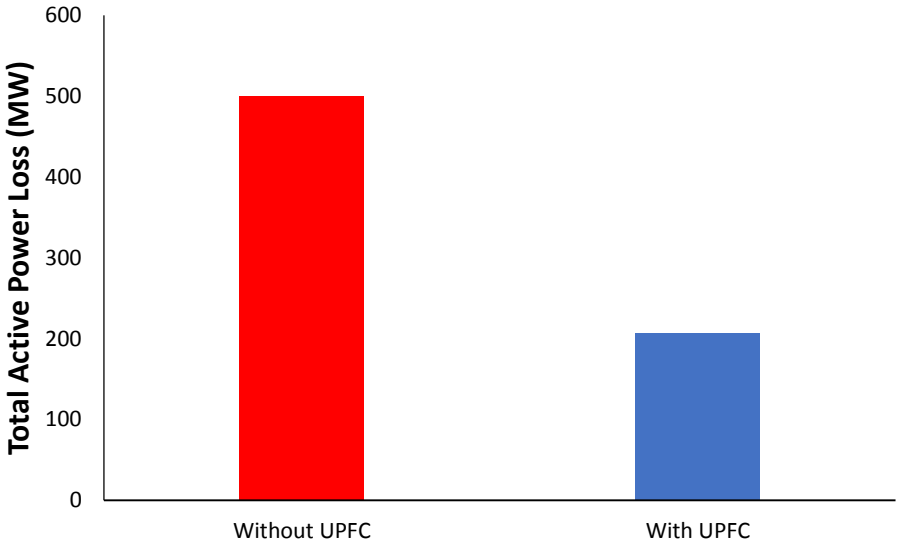

Figure 7: Comparison of total active power loss without and with optimally placed UPFC device on the IEEE 30-bus power system network

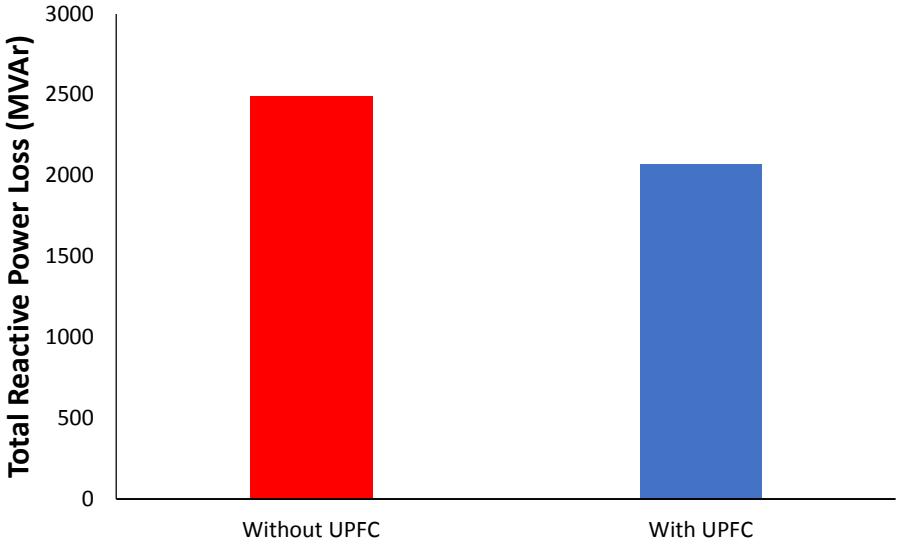

Figure 8: Comparison of total reactive power loss without and with optimally placed UPFC device on the IEEE 30-bus power system network

From Figure 5, the optimum point for UPFC placement as obtained from the load flow results was line 12-13. This is where the least active power loss was observed. The bus voltage magnitudes of all the buses in per unit were within the statutory limit defined by $0.95 \leq V \leq 1.10$pu without and with optimally placed UPFC device on line 12-13. From Figure 6, it was observed that without compensation applied to the test network, the voltage magnitude of all the buses were within the statutory limit, while with optimally placed UPFC device, the voltage magnitude of some of the buses already within the statutory limit were further enhanced. The voltage of buses 10, 12, 14, 15, 16, 17, 18, 19, 20, 21, 22, 23, 24 and 26 increased from 0.9957, 0.9946, 0.9817, 0.9806, 0.9876, 0.9877, 0.9731, 0.9720, 0.9771, 0.9797, 0.9899, 0.9793, 0.9819, 0.9927 to 1.0266, 1.0500, 1.0478, 1.0384, 1.0423, 1.0259, 1.0220, 1.0154, 1.0174, 1.0162, 1.0206, 1.0174, 1.0120, and 1.0109 respectively. From Figure 7, the total active power loss on IEEE 30-bus network was 499.10 MW without compensation, and reduced to 206.40 MW with optimally placed UPFC, equivalent to a percentage improvement of 58.65 %. Similarly, from Figure 8, the total reactive power loss was 2488.70 MVAr without compensation and decreased to 2067.20 MVAr with UPFC optimally placed showing an improvement of 16.94 %.

The load flow results obtained from [16], [17] among others who have also employed PSO based UPFC placement for power system loss minimization using some other practical networks as case studies, reviewed that there is reduction in active and reactive power losses and enhancement of voltage profile which is in line with the results obtained from this study.

IV. CONCLUSION

FACTS technology has been proven as a new way of utilizing the existing available power capacity, and can increase the system load ability, enhance the voltage profile, and ensure the constraints of the power system network falls within its statutory limit. This study employed PSO based UPFC placement for power system loss minimization using IEEE 30-bus system as a case study. The simulation results showed that PSO is a useful and suitable technique that could be deployed to find the optimum location for FACTS compensating devices such as UPFC to achieve an improved power system performance.

REFERENCES

[1]. K. Lokanadham, "Optimal Location of FACTS Devices in Power System by Genetic Algorithm," Global Journal of Researches in Engineering, vol. 10, no. 1, pp. 25-30, 2010.
[2]. T.R. Ayodele, A.S. Ogunjuyigbe, and O.O. Oladele, "Improving the transient stability of Nigerian 330kv Transmission network using static var compensation part 1: The base study," Nigerian Journal of Technology, vol. 35, no. 1, pp. 155-166, 2016.
[3]. K.O. Oyedoja, "Modelling and Simulation Study of the Use of Static Var Compensator (SVC) for Voltage Control in Nigeria Transmission Network," International Journal of Engineering and Applied Sciences, vol. 5, no. 5, pp. 44-50, 2014.
[4]. B. Noor, M.A. Aman, M. Ali, S. Ahmed, and F.W. Karam, "Impact of Thyristor Controlled Series Capacitor on Voltage Profile of Transmission Lines using PSAT," International Journal of Advanced Computer Science and Applications, vol. 9, no. 2, pp. 306-310, 2018.
[5]. A. K. Mohanty, and A.K. Barik, "Power System Stability Improvement Using FACTS Devices," International Journal of Modern Engineering Research, vol. 1, no. 2, pp. 666-672, 2012.
[6]. J.B. Gupta, A Course in Power Systems, 10th edition, S.K. Kataria and Sons Publisher, New Delhi, India, 2011.

[7]. N. Namrata, "Congestion Management in Deregulated Power System using Facts Controller," International Journal of Engineering Research and General Science, vol. 2, no. 6, pp. 653-661, 2014.
[8]. P. Prasad, A. V. Reddy, and B. Reddy, "Power Loss Minimization in Distribution System using Network Reconfiguration with Particle Swarm Optimization," International Journal of Engineering Science and Advanced Technology, vol. 5, no. 3, pp. 171-178, 2015.
[9]. B. Bhattacharyya, V. K. Gupta, and S. Kumar, "Reactive Power Optimization with SVC & TCSC using Genetic Algorithm," Advances in Electrical and Electronic Engineering, vol. 12, no. 1, pp. 1-12, 2014.
[10]. H. Marefatjou, and I. Soltani, "Optimal Placement of STATCOM to Voltage Stability Improvement and Reduce Power Losses by using QPSO Algorithm," Journal of Science and Engineering, vol. 1, no. 1, pp. 1-20, 2013.
[11]. S.K. Joshi, and K.S. Pandya, "Influence of TCSC on social welfare and spot price – A comparative study of PSO with classical method," International Journal of Engineering, Science and Technology, vol. 2, no. 3, pp. 69-81, 2010.
[12]. S.A. Jumaat, I. Musirin, M.M. Othman, and H. Mokhlis, "Transmission Loss Minimization Using SVC Based on Particle Swarm Optimization," IEEE Symposium on Industrial Electronics and Applications, vol. 1, no.1, pp. 419-424, 2011.
[13]. A.A. Shehata, A. Refaat, M.K. Ahmed, and N.V. Korovkin, "Optimal placement and sizing of FACTS devices based on Autonomous Groups Particle Swarm Optimization technique," Archives of Electrical Engineering, vol. 70, no. 1, pp. 161-172, 2021.
[14]. I. I. Alnaib, "IEEE-Bus System Data," 2020. Available: ResearchGate, https://www.researchgate.net/publication/340183939_IEEE-BUS_SYSTEM_DATA. [Accessed June 2, 2023].
[15]. D. K. Dharamjit, and D. K. Tanti, "Load Flow Analysis on IEEE 30 bus System," International Journal of Scientific and Research Publications, vol. 2, no. 11, pp. 1-6, 2012.
[16]. P.H. Krishna, and S.V. Reddy, "Optimal Location of UPFC for Voltage Stability using Particle Swarm Optimization," International Journal of Innovative Research in Technology, vol. 1, no. 11, pp. 232-238, 2014.
[17]. R. A. Amer, G. A. Morsy, and E. Saad, "Optimal Power Flow Problem Solution Incorporating FACTS Devices Using PSO Algorithm," Engineering Research Journal, vol. 36, no. 4, pp. 357-366, 2013.

APPENDICES

APPENDIX I: The parameter value used for the PSO

PSO Parameter	**Value**
c_1	0.1
c_2	0.2
r_1	0 to 1
r_2	0 to 1
w_{max}	0.8
w_{min}	0.2
Population size (N)	10
Maximum number of iterations	100

APPENDIX II: Parameters used for UPFC Design/Sizing

UPFC Parameters	IEEE 30 Bus
Is	16
Ir	17
Xvr	0.1
Xcr	0.1
Vvrtarget	1.0
Vstat	1
Psp	0.4
Qsp	0.02
Pstat	1
Qstat	1
Flow	[-1]
Vcr	0.04
Vvr	1.0
Vvrmax	1.1
Vvrmin	0.9
Vcrmax	0.2
Vcrmin	0.001
Tvr	0.0
Tcr	[-87.13/57.3]